

## MEASUREMENTS OF ELASTIC MODULUS IN ZR ALLOYS FOR CANDU APPLICATIONS

Z.L. Pan<sup>1</sup>, N. Wang<sup>2</sup> and Z. He<sup>2</sup>

<sup>1</sup>Materials and Mechanics Branch and <sup>2</sup>Fuel Development Branch  
Atomic Energy of Canada Limited, Chalk River Laboratories  
Chalk River, Ontario, Canada, K0J 1J0

**ABSTRACT** - Measurements of elastic modulus as a function of temperature from 20 to 400°C were carried out on specimens of Zr-2.5Nb, Zircaloy-4, Zircaloy-2 and Excel Zr alloy using an ultrasonic resonance technique. The specimens were machined from CANDU pressure tubes, a calandria tube and commercial sheet material. Effects of crystallographic texture, neutron irradiation and hydrogen on elastic modulus were investigated. The results show that elastic modulus of the Zr alloys (1) decreases with increasing temperature, (2) depends strongly on crystallographic texture, and (3) increases slightly with neutron irradiation.

### 1. Introduction

Most of the core components of a CANDU<sup>1</sup> reactor are made of Zr alloys, such as Zr-2.5Nb for pressure tube, Zircaloy-2 for calandria tube and Zircaloy-4 for fuel bundle etc. The elastic modulus is an intrinsic material property and its precise measurement is required over the operating temperature range of a CANDU reactor for engineering assessments. In the early 1970s, AECL measured the elastic modulus of several Zr alloys [1, 2]. The specimens used in these early measurements were prepared from Zr-2.5Nb bar and plate rather than the produced form (tubes) used in CANDU reactors. In addition, the orientation dependence of the elastic modulus was not determined. More recently the Canadian Standard Association (CSA) has issued CSA N285.6-05 [3], which provides elastic modulus of Zr-2.5Nb and Zircaloy-2, but not for Zircaloy-4. The reason for the differences between the previous measurements [1, 2] and values given by N285.6-05 are reviewed. The focus of the present investigation is to determine the elastic modulus of several zirconium alloys over a temperature range of 20 - 400°C.

Elastic strain of a solid is defined as the completely recoverable and instantaneous strain resulting from an applied stress. The constitutive equations, i.e. generalized Hooke's law [4], provide a relationship between stress and strain for a linear-elastic solid:

$$\sigma_{ij} = C_{ijlm} \varepsilon_{lm} \quad (1)$$

where  $\sigma_{ij}$  and  $\varepsilon_{lm}$  are the stress and strain tensors, respectively, and  $C_{ijlm}$  is the elastic constants tensor. For an isotropic solid only two elastic constants are independent: Young's modulus  $E$  for dilatational strain and shear modulus  $G$  for shear strain, both are termed "Elastic Moduli". Another elastic constant Poisson's ratio  $\nu = E/2G - 1$  can be deduced from values of elastic moduli  $E$  and  $G$ . From equation (1), the elastic moduli are defined as the slopes of stress – strain

---

<sup>1</sup> CANDU is a registered trademark of Atomic Energy of Canada Limited (AECL).

curves within the elastic limit. Young's modulus and shear modulus can be determined from a tensile test and torsional test, respectively. Such direct measurement of elastic modulus from a stress - strain curve is called the "Static Elastic Modulus". Since the elastic limit of strain is low, usually  $< 0.1\%$  for most engineering materials, the accuracy of the static method is generally poor (error  $> \pm 10\%$ ). This is also a destructive test, and requires a minimum of one specimen per test. It is not surprising that various experimental techniques have been developed to determine the elastic moduli of materials. Most of these techniques use a sonic or ultrasonic resonance method as recommended by ASTM Standards, such as E 1875-00 for resonance method [5] and E 494-89 for ultrasonic pulse method [6]. The elastic modulus determined using a resonance or pulse technique is called "Dynamic Elastic Modulus (DEM)". The dynamic method is nondestructive and one specimen can be tested over a wide temperature range. These dynamic techniques require only very small strains,  $\sim 0.001\%$  and have a great precision in the measurement of elastic modulus. Such small strain avoids any intrinsic interference, e.g. viscoelasticity and stress relaxation etc., particularly at elevated temperatures. Theoretically, static tests give the isothermal elastic moduli, while dynamic tests give the adiabatic elastic moduli. Theoretical analysis [7] has indicated that the difference between isothermal elastic modulus and adiabatic elastic modulus is generally small, of the order of 1% of the static elastic modulus. Experimental results [8] have also confirmed this difference to be smaller than the uncertainty of measurements in static elastic modulus.

## 2. Experiments

### 2.1 Experimental Technique

Young's modulus was determined using the Automated Piezoelectric Ultrasonic Composite Oscillator Technique (APUCOT), which was developed by AECL to measure the elastic modulus and internal friction in pressure tubes, feeder pipe steels and other materials. The APUCOT is essentially a sonic resonance technique as described in ASTM E 1875-00, but its resonant bar is a composite structure containing four components: two quartz crystals, a fused quartz thermal buffer rod and a specimen. A schematic of this apparatus is shown in Figure 1. One of the quartz crystals is used to drive the composite oscillator, while the other is a passive pickup crystal to gauge the resonance response. The fused quartz rod is inserted between quartz crystals and the specimen to isolate the hot specimen from the cold quartz crystals, which are maintained at approximately room temperature. The composite oscillator assembly is mounted in a vacuum chamber. A detailed description of the APUCOT has been given elsewhere [9-11]. The length of the cylindrical (or rectangular) specimen must be determined prior to the test because both quartz crystals and fused quartz rod have been precisely matched for longitudinally resonating at a frequency of 40 kHz. The specimen must be machined to the required length to achieve this resonance frequency of 40 kHz in the entire composite oscillator assembly. To generate the optimum resonance, the specimen length must be an odd multiple of the half wavelength of the longitudinal standing wave at 40 kHz. From the elastic theory of solids, Young's modulus  $E$  is correlated with the longitudinal resonance frequency  $f$ , wavelength (= double length  $2l$  of specimen), and density  $\rho$  of the specimen with the following equation [11, 12]:

$$E = \frac{\rho}{A_n} \left( \frac{2lf}{n} \right)^2 \quad (2)$$

where  $n$  is the overtone mode number ( $n = 1$  for basic monotone;  $n = 3$  for the 3<sup>rd</sup> overtone and so on), and  $A_n$  is Raleigh's correction factor for specimen dimensions. The value of  $A_n$  is close to one if the cross section dimensions are smaller than the specimen length, such as  $< 1/10$  [12]. For the present specimens,  $A_1 = 0.9998$ . Tests were conducted with a heating rate of 1 or 2°C/min from 20 to 400°C. The specimen chamber was evacuated to a pressure of  $\sim 3 \times 10^{-3}$  torr ( $\sim 0.4$  Pa). The error in the temperature measurements was determined to be  $\pm 1^\circ\text{C}$ . Raw data of voltage, frequency and temperature were acquired every 6 seconds, which corresponds to a temperature range of 0.1 or 0.2°C. The average Young's modulus and temperature was recorded for every 1°C. Each specimen was thermal cycled five times. The tests were reproducible with a standard deviation of  $\leq \pm 0.1\%$  for Young's modulus at a given temperature.

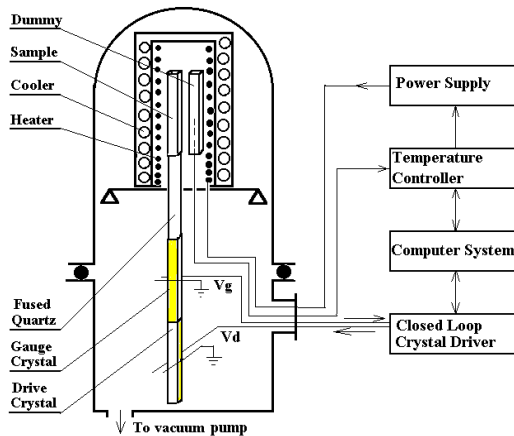


Figure 1 A schematic diagram of the APUCOT.

Archimedes method was used to determine the density of some specimens but for others the density was calculated from measurements of specimen dimensions and mass. These measurements were taken at room temperature and used to calculate  $E$  at elevated temperatures. It was estimated that the error in Young's modulus due to ignoring thermal expansion at high temperatures, 400°C, should be below 0.03% for Zr alloys. However, the error in the dimensions and mass measurements are approximately  $\pm 0.2\%$  and  $\pm 0.01\%$ , respectively, which results in an error of  $\pm 0.6\%$  in the density measurements. Using Archimedes method, the error in the density measurements is  $< \pm 0.5\%$ . Given the high stability of quartz crystals, the APUCOT can create a high accuracy in measurements of resonance frequency with an error  $< \pm 0.01\%$ . From these errors, the accuracy of Young's modulus is estimated to be  $\pm 1\%$ .

## 2.2 Specimens and Materials

For Zr-2.5Nb, the Young's modulus was determined over a range of temperature using material from several pressure tubes. A representative measurement was carried out on Pressure Tube #1912. The tube is considered as a representative of pressure tubes manufactured in the 1980s.

A piece of material  $\sim 3'' \times 3''$  was cut from this tube and then flattened. After flattening the material was annealed at  $400^{\circ}\text{C}$  for 24 hours for stress-relieving. Five specimens were machined from the plate at five different orientations of  $0^{\circ}$ ,  $22.5^{\circ}$ ,  $45^{\circ}$ ,  $67.5^{\circ}$  and  $90^{\circ}$  relative to the longitudinal direction (LN) of the tube, (Figure 2 right). The dimensions of the specimens are 45.5 mm (length)  $\times$  3.2 mm (thickness)  $\times$  2.8 mm (width), where the thickness corresponds to the radial direction of the parent tube. Specimens were also machined from pressure tubes that were not flattened as shown in Figure 2 (left). All of these specimens have a longitudinal orientation.

All Zircaloy-4 specimens were prepared from a commercial sheet, which was used to produce the end plate of CANDU fuel bundles. Using a low speed diamond saw, specimen T (transverse) was cut vertical to the rolling direction of the parent sheet, while specimen L (longitudinal) was cut along the rolling direction. Two heat treatments were, respectively, applied to the specimens: (1)  $\beta$ -heat treatment at  $1100^{\circ}\text{C}$  to obtain the Widmanstatten microstructure, which simulated the braze area of the end plate for CANDU fuel bundle; (2) The recrystallization annealing was at  $750^{\circ}\text{C}$ , held for 4 hours and then cooled in a furnace to establish the behaviour of the weakest part of the fuel sheath. Lastly, specimens were tested in the as-received conditions which was cold-worked and stress-relieved (CWSR). In the 1970s and 1980s, AECL developed a Zr alloy, termed "Excel", which contains 3.5% Sn, 0.8% Nb and 0.8% Mo [13]. Excel has a high strength and a high resistance to creep and irradiated growth. The material has been selected as a potential candidate for the CANDU – Supercritical Water Reactor (SCWR) pressure tube [14]. For this investigation specimens (longitudinal and transverse) were machined from the annealed Excel pressure tube #601. The metallurgical conditions of this tube have been given elsewhere [13, 14]. Zircaloy-2 specimens were machined from an off-cut of calandria tube IAI-6 along the longitudinal direction. All specimen parameters and some results are listed in Table 1.

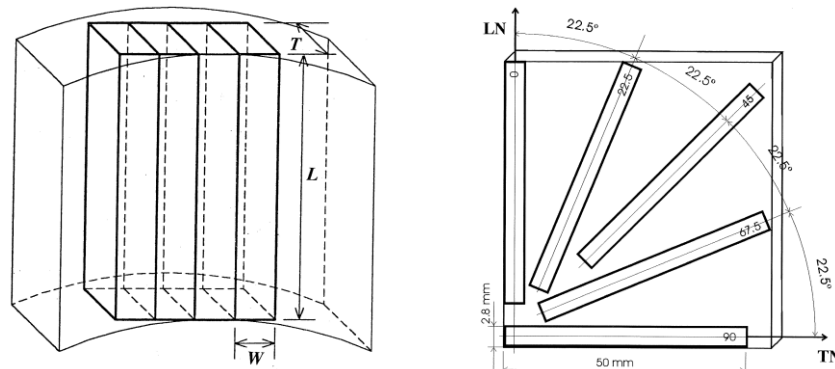


Figure 2 Samples machined from a piece of tube (left) or from a flattened piece of tube (right).

### 3. EXPERIMENTAL RESULTS

#### 3.1 Zr-2.5Nb pressure tube and the texture effect

Measurements of Young's modulus  $E$  as a function of temperature for five Zr-2.5Nb samples with different orientations are shown in Figure 3. The polynomial equation fit to the experimental data yields the following:

$$E = 96.771 - 0.04683T - 6.903 \times 10^{-5}T^2 + 7.350 \times 10^{-8}T^3 \quad \text{for } 0^\circ \quad (3)$$

$$E = 94.028 - 0.04763T - 3.233 \times 10^{-5}T^2 + 1.234 \times 10^{-8}T^3 \quad \text{for } 22.5^\circ \quad (4)$$

$$E = 91.757 - 0.04254T - 1.763 \times 10^{-5}T^2 + 1.351 \times 10^{-8}T^3 \quad \text{for } 45^\circ \quad (5)$$

$$E = 97.684 - 0.03676T - 1.856 \times 10^{-5}T^2 + 1.427 \times 10^{-8}T^3 \quad \text{for } 67.5^\circ \quad (6)$$

$$E = 103.88 - 0.02794T - 5.288 \times 10^{-5}T^2 + 5.972 \times 10^{-8}T^3 \quad \text{for } 90^\circ \quad (7)$$

where  $T$  is in °C,  $E$  is in GPa and the correlation coefficient is  $R^2 > 0.99994$ . The equations (3) to (7) are for specimens with  $0^\circ$ ,  $22.5^\circ$ ,  $45^\circ$ ,  $67.5^\circ$  and  $90^\circ$  orientations. For comparison with previous results [1, 2], a linear equation has been fit to data for the longitudinal and transverse samples. The linear equations describing the variation in  $E$  with  $T$  are:

$$E = 97.928 - 0.0647T \quad \text{for } 0^\circ \text{ present work} \quad (8)$$

$$E = 104.65 - 0.0407T \quad \text{for } 90^\circ \text{ present work} \quad (9)$$

$$E = 97.3 - 0.06T \quad \text{for } 0^\circ \text{ from [1]} \quad (10)$$

$$E = 95.9 - 0.0574T \quad \text{for } 0^\circ \text{ from [2]} \quad (11)$$

where  $T$  is in °C,  $E$  is in GPa and the correlation coefficients is  $R^2 = 0.998$  for equations (8) and (9). A comparison of the present measurements of equations (3) and (7) with previous results from [1, 2] and data provided in N285.6.7-05 [3] is shown in Figure 4.

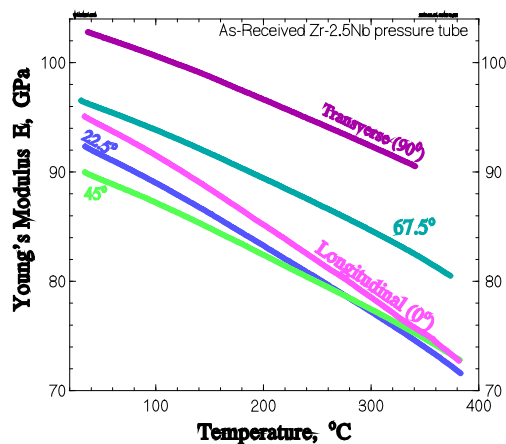


Figure 3 Young's modulus as a function of temperature in a Zr-2.5Nb tube at different orientations.

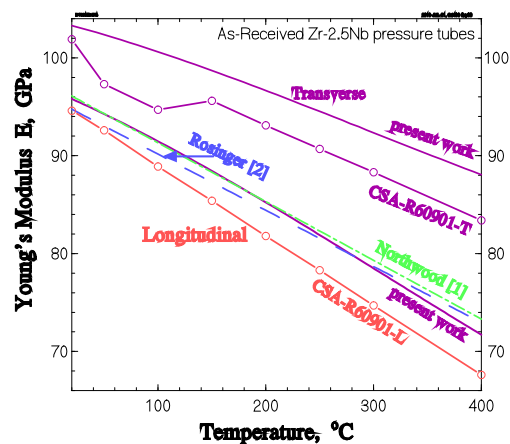


Figure 4 A comparison of the present work with previous results [1, 2] and CSA data [3].

The Longitudinal Young's modulus from the present investigation agrees with Northwood's line [1] at  $T < \sim 250^{\circ}\text{C}$ . However, at higher temperatures the newer data falls below the line given by [1]. In both the longitudinal and transverse directions, values of Young's modulus given in N285.6-05 are lower than the present results and Northwood's work. It should be noted that two data of Young's modulus given in CSA standard for the transverse direction at  $50^{\circ}\text{C}$  and  $100^{\circ}\text{C}$  are unexpectedly low. From equations (8) and (9), the rate of the decrease in Young's modulus with temperature, i.e. "temperature coefficient of Young's modulus", is different, i.e.  $0.0647$  and  $0.0407$  GPa/ $^{\circ}\text{C}$ , respectively, in the two orientations. Both lines of equations (10) or (11) from [1, 2] give higher values of elastic modulus at  $T > \sim 250^{\circ}\text{C}$  than the present work.

The variation in Young's modulus with orientation for the five samples tested at  $20$ ,  $200$  and  $400^{\circ}\text{C}$  is shown in Figure 5. To investigate the relationship between elastic modulus and crystallographic texture, the preferred orientation of basal pole  $\{0002\}$  in pressure tube #1912 was determined by the direct pole figure method using the X-ray diffraction technique [15]. The results from these measurements are shown in Figure 6. The Karn's orientation parameter  $f$  [16] is the volume fraction of crystals having basal poles oriented in one of the principal directions, i.e. longitudinal, transverse and radial of the tube, respectively denoted as  $f_l$ ,  $f_t$  and  $f_r$ . Using the basal pole texture data, the three Karn's parameters were calculated to be  $0.03$ ,  $0.63$  and  $0.34$ . It is evident that the predominant orientation of the basal pole is along the direction of the tube circumferential, i.e. transverse direction.

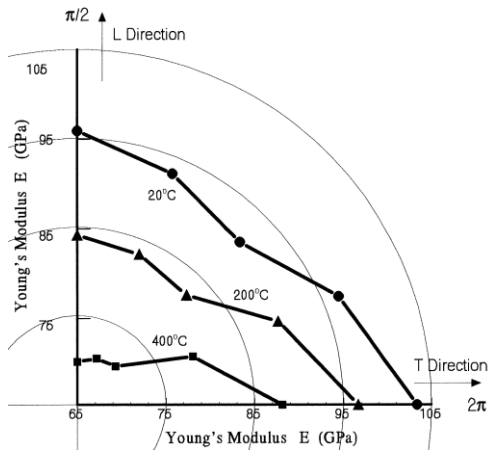


Figure 5 A polar plot of Young's modulus (radius length in GPa) versus orientation at  $20^{\circ}\text{C}$ ,  $200^{\circ}\text{C}$  and  $400^{\circ}\text{C}$  in tube #1912.

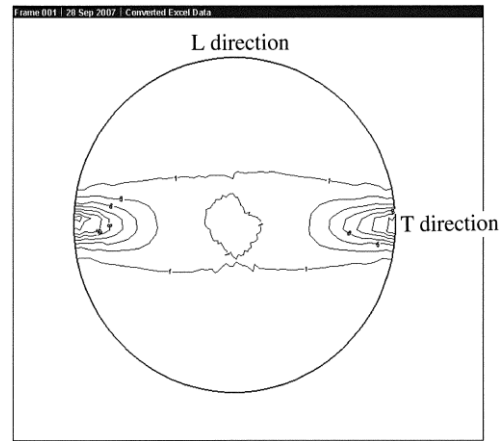


Figure 6  $\{0002\}$  pole figure of texture determined using X-ray diffraction in pressure tube #1912.

Fisher et al [17] reported five independent elastic constants for an  $\alpha$ -Zr single crystal. The highest value was  $c_{33}$  ( $= 1.649 \times 10^{12}$  dynes/cm $^2$ ) parallel to the basal pole direction  $[0001]$ . In the other directions the elastic constants were lower. In Zr-2.5Nb pressure tubes, the basal pole for the majority of  $\alpha$ -Zr crystals is preferentially orientated to the transverse direction of the tube. Thus, the highest value of measured elastic modulus should be along this direction. To calculate the mechanical properties of polycrystalline aggregates, Tomé et al [18] developed a self-consistent model, which takes into account the grain interaction and texture. Using this

model, the orientation dependence of Young's modulus was calculated at several temperatures using the texture measurements for a Zr-2.5Nb pressure tube. The calculated results are close to measured data, as shown in Figure 7. This is the evidence to confirm the orientation dependence of elastic modulus in pressure tubes is consistent with crystallographic texture of the tube. In operating pressure tubes, the orientation dependence of elastic modulus will result in an influence on the irradiation-induced deformation.

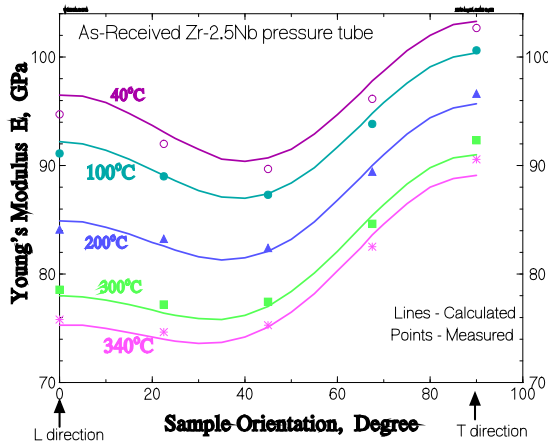


Figure 7 A comparison of calculated results of E vs. orientation with measured results.

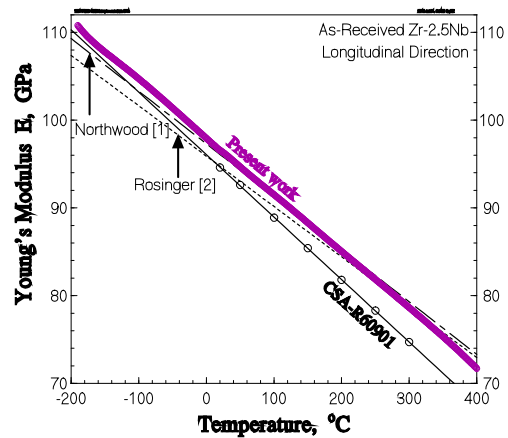


Figure 8 Elastic modulus of Zr-2.5Nb at low temperature range.

A Zr-2.5Nb specimen with the longitudinal direction was tested in the low temperature range of liquid nitrogen during warming up, and the result is shown in Figure 8. The curve of E versus T at the low temperature can be coincided with the curve beyond room temperature. It appears that the extrapolated lines of equations (10) and (11) from [1, 2] and from CSA give lower values of Young's modulus at the range of low temperature.

### 3.2 Effects of hydrogen and irradiation

Several specimens were machined from Zr-2.5Nb pressure tube R766 along the longitudinal direction, and then, were doped with hydrogen, the preparations of specimens have been described in detail elsewhere [10]. Elastic modulus as a function of temperature was determined in these specimens containing different concentrations of hydrogen, shown in Figure 9. It has been confirmed [10, 19] that a "knee" point in a plot of elastic modulus versus temperature is associated with the dissolution of hydride during heating or with the precipitation of hydride during cooling in a Zr alloy. The knee point can be used to identify the temperature of terminal solid solubility (TSS) of hydrogen in the Zr alloy. In the temperature range below the knee point in Figure 9, all E versus T lines coincide with each other, while in the temperature range beyond the TSS temperature, the level of E versus T lines decreases with increasing hydrogen concentrations in the Zr-2.5Nb specimens. The addition of hydrogen can depress the elastic modulus of the solid solution of Zr-H alloys. Same phenomenon was found in Excel Zr alloy [20]. However, the solid hydride  $\delta$ -ZrH<sub>1.5</sub> containing 60 at. % hydrogen is different from usual

$\alpha$ -Zr-H alloy. The curve of  $E$  versus  $T$  in  $ZrH_{1.5}$  reveal a non-monotonic feature in the range of 20 to 400°C due to the presence of a large internal friction peak. Experimental results and specimen preparation of solid hydrides have been given elsewhere [21, 22].

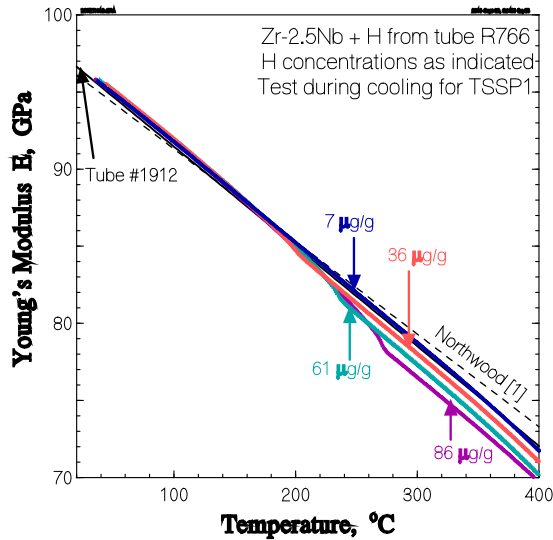


Figure 9 Effect of hydrogen on curves of  $E$  versus  $T$  in Zr-2.5Nb+H during cooling.

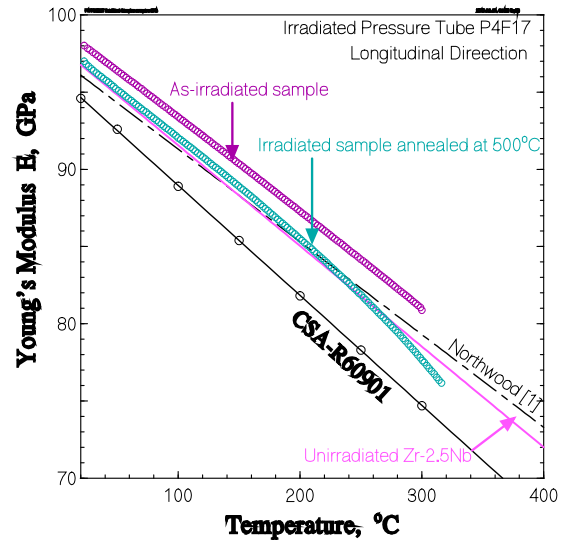


Figure 10 Elastic modulus in irradiated and annealed at 500°C Zr-2.5Nb.

A specimen was machined from an ex-service pressure tube P4F17 at the axial location close to the inlet burnish mark. The effective full power hours for this pressure tube was 15,090 h. At the axial location of this specimen, the neutron fluence was, approximately,  $1.3 \times 10^{25} \text{ n/m}^2$  ( $E > 1 \text{ MeV}$ ). Experimental results of  $E$  versus  $T$  curves for the irradiated specimen and for the same specimen after annealing at 500°C for 4 hours are shown in Figure 10. The purpose of the high temperature anneal is to recover the radiation damage. It appears that there is a small increase in Young's modulus with irradiation. Data from the annealed specimen falls close to the data for unirradiated pressure tube material. Given the limited number of tests reported here, additional experiments are required to verify if the Young's modulus is enhanced by neutron irradiation.

### 3.3 Zircaloy-4 – Endplate of Fuel Bundle

Measurements of Young's modulus as a function of temperature in the six specimens are plotted in Figure 11. In as-received (CWSR) specimens, a difference in Young's modulus between longitudinal (CL) and transverse (CT) orientations is evident in the experimental temperature range from 20 to 400°C. For other two groups of specimens (recrystallization and  $\beta$ -treated), the difference of Young's modulus between the two orientations is not significant in the same temperature range, such as curves RL versus RT, and WL versus WT in Figure 11. The  $\beta$ -treated specimens with Widmanstatten microstructure show a higher value of Young's modulus, while the recrystallization specimens have a relatively low value of Young's modulus over the whole temperature range. Polynomial equations fit to the experimental data yield the following relationships for  $E$  versus  $T$  for the CWSR specimens:

$$E = 97.355 - 0.05107T - 4.076 \times 10^{-5}T^2 + 2.208 \times 10^{-8}T^3 \quad \text{for longitudinal Zircaloy-4 (12)}$$

$$E = 98.441 - 0.04571T - 3.321 \times 10^{-5}T^2 + 1.666 \times 10^{-9}T^3 \quad \text{for transverse Zircaloy-4 (13)}$$

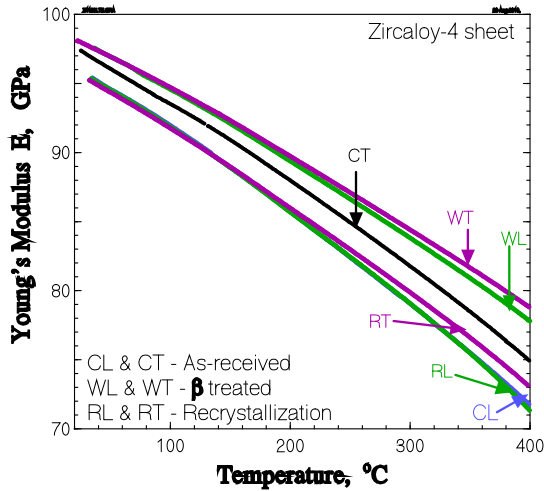


Figure 11 Young's modulus in Zircaloy-4 in 3 conditions of 2 directions.

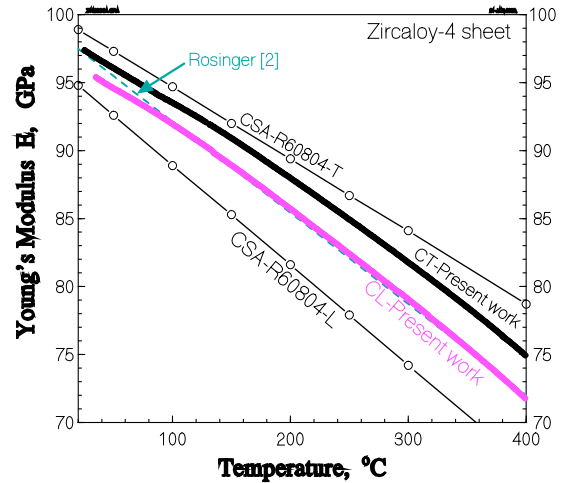


Figure 12 A comparison of Young's modulus in as-received Zircaloy-4.

where  $E$  is in GPa,  $T$  is in °C and the correlation coefficient is  $R^2 = 0.99997$ . A comparison of Young's modulus in as-received specimens with the data given by CSA Standard for alloy R60804 and by reference [2] for Zircaloy-4 is plotted in Figure 12. R60804 Seamless Tube is a commercial product of Zircaloy-4. The present experimental results are similar to the equations from reference [2] for the longitudinal orientation. Neither the elastic modulus in the transverse direction nor for heat treated material is provided in reference [2]. The present experimental results are slightly lower than CSA values [3] for transverse specimens and slightly higher than CSA values for longitudinal specimens, see Figure 12. This difference may be attributed to differences in the heat treatment conditions for specimens. The manufacturer of Zircaloy-4 [23] determined the Poisson's ratio in Zircaloy-4 to be from 0.406 at 24°C to 0.412 at 316°C and concluded the value of Poisson's ratio in Zircaloy-4 is nearly temperature independent in the temperature range.

### 3.4 Excel Zr Alloy Pressure Tube

The variations in Young's modulus with temperature for the longitudinal and transverse directions of an Excel pressure tube are plotted in Figure 13. Data from a Zr-2.5Nb pressure tube are included for comparison. The Young's modulus of Excel in the transverse direction agrees with the Zr-2.5Nb tube between 20 and 400°C. In the longitudinal direction the Young's modulus of Excel is slightly lower, ~6% less. Polynomial equations fit to the data yield:

$$E = 93.640 - 0.05434T - 7.848 \times 10^{-6}T^2 - 1.407 \times 10^{-8}T^3 \quad \text{for longitudinal Excel (14)}$$

$$E = 105.24 - 0.03324T - 3.333 \times 10^{-5}T^2 - 3.09 \times 10^{-8}T^3 \quad \text{for transverse Excel (15)}$$

where  $E$  is in GPa,  $T$  is in °C, and the correlation coefficient is  $R^2 = 0.99996$ . A previous work [20] conducted hydrogen ingress experiments at a constant temperature in the Ni-coated Excel specimens using the elastic modulus technique. It was shown that the variation of elastic modulus with the hydrogen ingress time can be used to reveal the start of hydride precipitation.

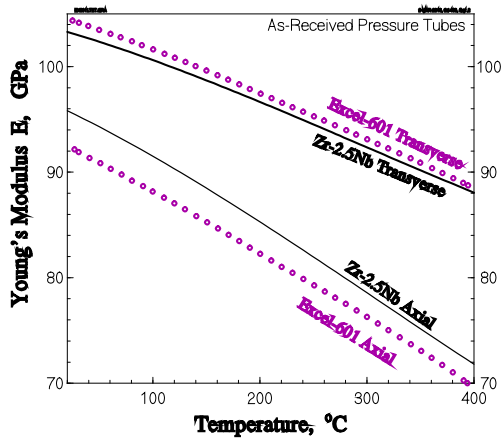


Figure 13 Elastic modulus in Zr alloy Excel.

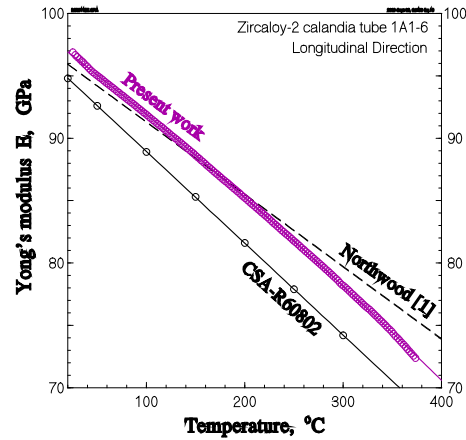


Figure 14 Elastic modulus in Zircaloy-2.

### 3.5 Zircaloy-2 – Calandria Tube

Young's modulus between 20 and 380°C for Zircaloy-2 specimen in the longitudinal orientation is included in Figure 14. A polynomial equation fit to this data yield the following equation:

$$E = 98.37 - 0.06595T - 1.33 \times 10^{-5}T^2 - 5.902 \times 10^{-8}T^3 \quad \text{for longitudinal Zircaloy-2} \quad (16)$$

where  $E$  is in GPa,  $T$  is in °C, and the correlation coefficient is  $R^2 = 0.99996$ . In Figure 14, the present experimental result is compared with lines from [1] for Zircaloy-2 and from CSA N285.6 [3] for R60802 seamless tubes. It can be seen that the present result is consistent with Northwood's work [1] and higher than the CSA data. However, CSA Standard N285.6 does not indicate any difference in elastic modulus between both materials of Zircaloy-2 (R60802) and Zircaloy-4 (R60804), and between both treatments of annealed tubes and extruded tubes.

## 4. CONCLUSIONS

The elastic modulus as a function of temperature was determined for specimens of Zr-2.5Nb and Excel pressure tubes, Zircaloy-4 fuel bundle endplate, Zircaloy-2 calandria tube from 20°C to 400°C. The effects of temperature, crystallographic texture, hydrogen and neutron irradiation on the elastic modulus were investigated. The results show that elastic modulus decreases with increasing temperature and depends strongly on the crystallographic texture of Zr alloys parent

material. From a limited number of measurements, determined elastic modulus in an irradiated pressure tube appears to be slightly higher than that of unirradiated specimens.

## **5. REFERENCES**

- [1] D.O. Northwood, I.M. London and L.E. Bahen, “Elastic constants of zirconium alloys”, J. Nucl. Mat. Vol.55, 1975, pp.299-310.
- [2] H.E. Rosinger and D.O. Northwood, “The elastic properties of zirconium alloy fuel cladding and pressure tubing materials”, J. Nucl. Mat., Vol.79, 1979, pp.170-179.
- [3] Canadian Standards Association, “Material standards for reactor components for CANDU nuclear power plants”, N285.6 Series-05, July, 2005, p.37.
- [4] W. Pfeiler, “Alloy Physics”, Chapter 4.2 and section 11.2.3, Willey-VCH Verlag GmbH & Co. KGaA, Weinheim, 2007, p. 126 and p. 598.
- [5] ASTM Standards, E 1875-00, “Standard Test Method for Dynamic Young’s Modulus, Shear Modulus, and Poisson’s Ratio by Sonic Resonance”, Annual Book of ASTM Standards, ASTM, Philadelphia, PA, Vol. 03.01, 2000.
- [6] ASTM Standards, E 494-89, “Standard Practice for Measuring Ultrasonic Velocity in Materials”, Annual Book of ASTM Standards, ASTM, Philadelphia, PA, Vol. 03.03, 2000, pp. 176-187.
- [7] H.G. Huntington, “The Elastic Constants of Crystals”, in “Solid State Physics”, Ed. by F. Seitz and D. Turnbull, Academic Press Inc. New York, 1958, Vol. 7, pp. 213 – 351.
- [8] M.Radovic, E. Lara-Curzio and L.Riester, “Comparison of Differential Techniques for Determination of Elastic Properties of Solids”, Mat. Sci. & Eng. Vol.A368, (2004) p. 56.
- [9] I.G. Ritchie, Z.L. Pan, K.W. Sprungann, H.K. Schmidt and R. Dutton, “High damping alloys – the metallurgist’s cure for unwanted vibrations”, Canadian Met. Quarterly, Vol. 26, 1987, pp. 239 – 250.
- [10] Z.L. Pan, I.G. Ritchie and M.P. Puls, “The terminal solid solubility of hydrogen and deuterium in Zr-2.5Nb alloys”, J. Nucl. Mat. Vol. 228, 1996, pp. 227–237.
- [11] L.S. Cook, A. Wolfenden and G.,M. Ludtka, “Longitudinal and Flexural Resonance Methods for the Determinations of the variation with Temperature of Dynamic Young’s Modulus in 4330V Steel”, in “Dynamic Elastic Modulus Measurements in Materials”, Ed. by A. Wolfenden, ASTM STP 1045, 1990, pp. 75-89.
- [12] I.G. Ritchie, H.E. Rosinger, A.J. Shilinglaw and W.H. Fleury, “The Dynamic Elastic Behaviour of a Fiber-reinforced Composite Sheet: I. The precise experimental Determination of the Principle Elastic Moduli”, J. Phys. D: Appl. Phys., Vol. 8, 1975, pp. 1733–1749.

- [13] C.E. Ells, C.E. Coleman, B.A. Cheadle, S. Sagat, D.K. Rodgers, "The Behaviour of Hydrogen in Excel Alloy", *J. Alloy Compounds*, Vol. 231 (1995), pp. 785-791.
- [14] Z.L. Pan, "Delayed Hydride Cracking and Elastic Properties of Excel, A Candidate CANDU-SCWR Pressure Tube Material", Proceedings of the Canadian Nuclear Society Conference "The 2<sup>nd</sup> Canada-China Joint Workshop on Supercritical Water-Cooled Reactors (CCSC-2010)" paper #54, April, 2010.
- [15] M. Griffiths, J. Mecke and J.E. Winegar, "Evolution of Microstructure in Zirconium Alloys during Irradiation", *Zirconium in Nuclear Industry*, 11<sup>th</sup> International Symposium, ASTM, STP 1295, (1996) pp.580-602.
- [16] J.J. Kearns, "Thermal Expansion and Preferred Orientation in Zircaloy", WAPD-TM-472, Report of Westinghouse Electric Corporation, Bettis Atomic Power Laboratory, Pittsburgh, PA, 1965 November.
- [17] E.S. Fisher and C.J. Renken, "Adiabatic Elastic Moduli of Single Crystal Alpha Zirconium", *J. Nucl. Mat.* Vol. 4, No.3, (1961), p. 311.
- [18] C.N. Tomé, C.B. So and C.H. Woo, "Self Consistent Calculation of Steady-State Creep and Growth in Textured Zirconium", *Phil. Mag.*, Vol. A67 (1993) pp. 917-930.
- [19] Z.L. Pan and M.P. Puls, "Precipitation and Dissolution Peaks of Hydride in Zr-2.5Nb during Quasistatic Thermal Cycles", *J. Alloys Compounds*, Vol. 310 (2000), pp. 214-218.
- [20] Z.L. Pan, M.P. Puls and I.G. Ritchie, "Measurements of Hydrogen Solubility during Isothermal Charging in a Zr Alloy using an Internal Friction Technique", *J. Alloys & Compounds* Vol. 211/212 (1994), pp. 245-248.
- [21] Z.L. Pan and M.P. Puls, "Internal Friction Peaks Associated with the Behaviour of Hydrogen in Zr and Zr-2.5Nb", *Materials Sci. & Eng.* Vol. A442 (2006), pp. 109-113.
- [22] M.P. Puls, S.Q. Shi and J. Rabier, "Experimental Studies of Mechanical Properties of Solid Zirconium Hydrides", *J. Nucl. Mat.* Vol. 336 (2005), pp. 73-80.
- [23] E.B. Schwenk, K.R. Wheeler, G.D. Sheater and R.T. Webster, "Poisson's Ratio in Zircaloy-4 between 24° and 316°C", *J. Nucl. Mat.*, Vol.73 (1978), pp. 129-131.

Table 1. Specimen's parameters and experimental results comparing with CSA [3] data

Material	Sample ID	Orientation	Density g/cm <sup>3</sup>	Young's modulus, GPa		Heat treatment	Comment
				at 20°C	at 300°C		
Zr-2.5Nb	W19125	Longitudinal	6.52	95.76	75.65	As-received	PT #1912
Zr-2.5Nb	W19124	22.5°	6.52	93.07	77.16	As-received	PT #1912
Zr-2.5Nb	W19123	45°	6.52	90.90	77.76	As-received	PT #1912
Zr-2.5Nb	W19122	67.5°	6.52	96.94	85.37	As-received	PT #1912
Zr-2.5Nb	W19121	Transverse	6.52	103.30	92.35	As-received	PT #1912
Zircaloy-4	Z4L1	Longitudinal	6.53	96.32	78.96	As-received	Endplate
Zircaloy-4	Z4T1	Transverse	6.53	97.51	82.19	As-received	Endplate
Zircaloy-4	Z4L2	Longitudinal	6.53	98.30	83.80	β-treatment	Endplate
Zircaloy-4	Z4T2	Transverse	6.53	98.21	84.40	β-treatment	Endplate
Zircaloy-4	Z4L3	Longitudinal	6.53	96.21	79.04	Recrystall.	Endplate
Zircaloy-4	Z4T3	Transverse	6.53	95.92	79.85	Recrystall.	Endplate
Excel Zr	E6011	Longitudinal	6.59	92.55	76.25	As-received	PT #601
Excel Zr	E6012	Transverse	6.59	104.56	91.43	As-received	PT #601
Zircaloy-2	D959	Longitudinal	6.50	97.79	75.79	As-received	CT-IAI-6
Zr-2.5Nb	F177	Longitudinal	6.52	98.18	80.99	Irradiated	PT#P4F17
Zr-2.5Nb	F177	Longitudinal	6.52	97.09	77.68	Annealed	PT#P4F17
Zr-2.5Nb	CSA-R60901	Longitudinal	N/A	94.6	74.7	As-received	Seamless tube
Zr-2.5Nb	CSA-R60901	Transverse	N/A	101.9	88.3	As-received	Seamless tube
Zircaloy-2	CSA-R60802	Longitudinal	N/A	94.8	74.2	Annealed	Seamless tube
Zircaloy-2	CSA-R60802	Transverse	N/A	98.9	84.1	Annealed	Seamless tube
Zircaloy-4	CSA-R60804	Longitudinal	N/A	94.8	74.2	Annealed	Seamless tube
Zircaloy-4	CSA-R60804	Transverse	N/A	98.9	84.1	Annealed	Seamless tube